HYDROGEN STORAGE IN CARBON SINGLE-WALL NANOTUBES

A.C. Dillon, K.E.H. Gilbert, P.A. Parilla, J.L. Alleman,
G.L. Hornyak, K.M. Jones, and M.J. Heben

National Renewable Energy Laboratory
Golden, CO 80401-3393

Abstract

Carbon single-wall nanotubes (SWNTs) and other nanostructured carbon materials have attracted considerable interest recently due to several reports of high hydrogen storage capacities at room temperatures. Other reports indicate room temperature storage capacities are ~ 0 wt%. All in all, the reported capacities on these materials range from 0 to 60 wt%. Careful work at NREL indicates a maximum capacity for adsorption of hydrogen on SWNTs is ~8 wt%. Samples displaying this maximum value were prepared by sonicating purified SWNTs in a dilute nitric acid solution with a high-energy probe. The process cuts the SWNT into shorter segments and introduces a Ti-6Al-4V alloy due to the disintegration of the ultrasonic probe. The Ti-6Al-4V alloy is a well-known metal hydride and its contribution to the measured hydrogen uptake must be accounted for in order to assess the amount of hydrogen stored on the SWNT fraction. One way to evaluate the relative importance of the cutting and the presence of the alloy in producing active SWNT materials is to produce cut samples that do not contain metal impurities. Metal hydrides may then be subsequently introduced in a controlled manner. This paper describes the experiments used to evaluate the hydrogen storage capacity of the sonicated SWNTs, and introduces new methods for cutting SWNTs that avoid the introduction of the impurity alloy. A Raman spectroscopy technique was also developed which enables the degree of cutting to be tracked. This year we also developed a method for growing SWNTs by chemical vapor deposition from methane that promises, when scaled-up, to produce SWNTs for approximately $1/kg. This latter work will not be discussed here, but will soon be submitted to the peer-reviewed literature.

Background

Interest in hydrogen as a fuel has grown dramatically since 1990, and many advances in hydrogen production and utilization technologies have been made. Hydrogen storage technology must be significantly advanced in performance and cost effectiveness if the U.S. is to establish a hydrogen-based transportation system. Hydrogen provides more energy than either gasoline or natural gas on a weight basis. It is only when the weight, volume, and round-trip energy costs of the entire fuel storage system and charging/discharging cycle is considered that hydrogen's drawbacks become apparent. New approaches enabling more compact, lightweight, and energy efficient hydrogen storage are required in order for the wide-spread use of hydrogen powered vehicles to become a reality.

Currently Available Hydrogen Storage Technologies

Hydrogen can be made available on-board vehicles in containers of compressed or liquefied H2, in metal hydrides, or by gas-on-solid adsorption. Hydrogen can also be generated on-board by reaction or decomposition of hydrogen containing species[2]. Although each method possesses desirable characteristics, no approach satisfies all of the efficiency, size, weight, cost and safety requirements for transportation or utility use. The D.O.E. energy density goals for vehicular hydrogen storage call for systems capable of storing hydrogen at 6.5 wt % H_2 and 62 kg H_2/m^3.

Gas-on-solid adsorption is an inherently safe and potentially high energy density hydrogen storage method that could be more energy efficient than chemical or metal hydrides and compressed gas storage. Consequently, the hydrogen storage properties of high surface area "activated" carbons have been extensively studied[3-5]. However, activated carbons are ineffective in hydrogen storage systems because only a small fraction of the pores in the typically wide pore-size distribution are small enough to interact strongly with gas phase hydrogen molecules.

Carbon single-wall nanotubes (SWNTs) and other nanostructured carbon materials have attracted considerable interest recently due to several reports of high hydrogen storage capacities at room temperatures. However, conflicting reports indicate that room temperature storage capacities do not exceed ~ 0 wt%. All in all, reported capacities range from 0 to 60 wt%. Qualitatively, these reports are categorized by the research community as follows; (i) those which are thought to be clearly un-physical with H/C ratios exceeding 2 (~ 14 wt% H), (ii) those which are consistent with expectations based on findings for activated and other, conventional high-surface area carbons (~ 0 wt% H), (iii) those which fall into the intermediate range (1 – 14 wt%) and are not obviously incorrect. Table 1 shows some of the data that has been reported organized by decreasing hydrogen storage weight density. A recent review paper discusses these results in more detail[6].

Our early experiments on un-purified SWNT samples indicated that 5 to 10 wt% hydrogen storage would be possible at room temperature[1]. Since then we have produced high purity SWNTs, and developed methods to activate them for hydrogen storage. A maximum value of ~ 8 wt% hydrogen has been measured for several different samples. These results have been the subject of considerable debate and scrutiny in the literature and questions remain regarding the role of an impurity metal alloy that is incorporated during high-energy ultrasonic probe sonication and the reproducibility of the results[7,8]. Careful, cross-calibration of the experimental apparatuses with three different standards establish the validity of the measurements[9], and repeated measurements on a given sample yield reproducible results, but nominally similar

sample preparation procedures do not repeatedly produce samples that exhibit the same hydrogen storage capacities. This may be attributed to the lack of control in the ultrasonic cutting and alloy incorporation process. The degree of tube cutting, and how, where, and in what form the metal particles are incorporated can vary dramatically even when identical sonication parameters are employed. Ideally a method that provides for detailed and independent control of both the cutting and metal incorporation should be employed. Towards this goal, we have developed a controlled cutting technique that does not simultaneously incorporate a metal hydride alloy. We have also developed a Raman spectroscopy technique that measures the extent of cutting and have demonstrated that similar degrees of cutting are achieved for identical conditions with the new cutting method. Future work will focus on developing methods for the controlled incorporation of metal alloy particles in discrete sizes and locations within the SWNT matrix.

Two-color Raman spectroscopy studies show that variation in material synthesis can lead to the formation of tube samples having differing chirality and diameter distributions. The types of tubes used in a given experiment may also influence the hydrogen adsorption capacities. Adsorption measurements on samples having differing distributions indicate a link between SWNT size and type and hydrogen capacity[10]. Last year we reported that materials generated with an alexandrite laser (755 nm) were more difficult to activate to high hydrogen storage capacities than samples fabricated with a Nd:YAG laser (1064 nm) even when all of the same sample purification, cutting and activation steps were taken. This year we have successfully generated tailored SWNTs with the alexandrite laser that are similar in both size and type to the SWNTs previously found to have high adsorption capacities. Although we have again demonstrated high hydrogen storage capacities on these tailored alexandrite materials, we are not yet able to generate samples that exhibit high hydrogen storage capacity in a repeatable fashion, presumably due to the lack of control in the sonication step.

Technical Approach and Summary of Past Work

We have been working on the idea that single wall carbon nanotubes could serve as ideal hydrogen adsorbents since 1993[11]. The concept was motivated by theoretical calculations[12] which suggested that adsorption forces for polarizeable molecules within SWNTs would be stronger than for adsorption on ordinary graphite. Thus, high H_2 storage capacities might be achieved at relatively high temperatures and low pressures as compared to adsorption on activated carbons.

In 1994 we presented microbalance data that demonstrated gravimetric hydrogen storage densities of up to 8.4 wt% at 82 K and 570 torr on samples containing carbon nanotubes[13]. This substantial uptake at low hydrogen pressures demonstrated the strong interaction between hydrogen and these materials, consistent with higher heats of adsorption than can be found with activated carbons.

In 1995, temperature programmed desorption (TPD) studies showed significant H_2 adsorption near room temperature[2]. The adsorption energies were estimated to be a factor of 2-3 times higher than the maximum that has been observed for hydrogen adsorption on conventional activated carbons. These were the first results that demonstrated the existence of stable adsorbed hydrogen on any type of carbon at temperatures in excess of 285 K.

Table 1: Compilation of reports of hydrogen storage on engineered carbon materials at room-temperature and above, as of 2001. Also included are a few data points for hydrogen storage investigations at lower temperatures. The data is more thoroughly discussed and the specific references can be found in reference 6.

Material	Density wt%	Temp (K)	Pressure (MPa)	Reference	Year
GNFs (herring bone)	67.55	RT	11.35	Chambers	1998
GNFs (platelet)	53.68	RT	11.35	Chambers	1998
Li-MWNTs	20	~473-673	0.1	Chen	1999
K-MWNTs	14	< 313	0.1	Chen	1999
GNFs (tubular)	11.26	RT	11.35	Chambers	1998
CNFs	~10	RT	10.1	Fan	1999
Li/K-GNTs (SWNT)	~10	RT	8-12	Gupta	2000
GNFs	~10	RT	8-12	Gupta	2000
SWNT (lo purity)	5-10	273	0.04	Dillon	1997
SWNT (hi purity)	8.25	80	7.18	Ye	1999
CN nanobells	8	573	0.1	Bai	2001
Nano graphite	7.4	RT	1	Orimo	2000
SWNT (hi purity + Ti alloy)	6-7	~300-700	0.07	Dillon	2000
GNFs	6.5	RT	~12	Browning	2000
CNFs	~5	RT	10.1	Cheng	2000
MWNTs	~5	RT	~10	Zhu	2000
SWNT (hi purity + Ti alloy)	3.5-4.5	~300-600	0.07	Dillon	1999
SWNT (50% purity)	4.2	RT	10.1	Liu	1999
Li-MWNTs	~2.5	~473-673	0.1	Yang	2000
SWNT (50% purity)	~2	RT	echem	Nutzenadel	1999
K-MWNTs	~1.8	< 313	0.1	Yang	2000
(9,9) array	1.8	77	10	Wang	1999
MWNTs	< 1	RT	echem	Beguin	2000
CNF	0.1-0.7	RT	0.1-10.5	Poirier	2001
(9,9) array	0.5	RT	10	Wang	1999
SWNTs	~0.1	300-520	0.1	Hirscher	2000
Various	< 0.1	RT	3.5	Tibbets	2001
SWNT (+ Ti alloy)	0	RT	0.08	Hirscher	2001

In 1996 we performed a detailed comparative investigation of the hydrogen adsorption properties of SWNT materials, activated carbon, and exfoliated graphite[14]. We determined the amount of hydrogen that is stable at near room temperatures on a SWNT basis is between 5 and 10 wt%, and found that an initial heating in vacuum is essential to remove pre-adsorbed species. Oxidation of SWNTs in H_2O improved the hydrogen storage capacity by more than a factor of three. We also utilized NREL's High Flux Solar Furnace to form nanotubes with concentrated sunlight for the first time.

In 1997, the desorption of hydrogen was found to fit 1st order kinetics as expected for un-dissociated H_2, and the activation energy for desorption was measured to be 19.6 kJ/mol[15]. This value is approximately five times higher than the value expected for desorption of H_2 from planar graphite. We also employed diffuse reflectance Fourier transform infrared spectroscopy to determine the concentrations and identities of chemisorbed species bound to the carbon surface as a function of temperature[16], and determined that “self-oxidation” allows high-temperature adsorption of hydrogen to occur in the arc-generated SWNT materials. We began synthesizing SWNT materials in much higher yield using the laser vaporization process developed by Smalley and co-workers[17], and determined that laser grown SWNTs could not be activated for high-temperature H_2 uptake by the same oxidative methods that were found to be effective for arc-discharge tubes.

In 1998 we made significant advances in synthesis and characterization of SWNT materials so that we could prepare gram quantities of SWNT samples and measure and control the diameter distribution of the tubes by varying key parameters during synthesis[18]. By comparing continuous wave and pulsed laser techniques, we learned that it is critical to stay in a vaporization regime in order to generate SWNTs at high yield. We also developed methods which somewhat purified the nanotubes and cut them into shorter segments. We performed temperature programmed desorption spectroscopy on high purity carbon nanotube material obtained from our collaborator Prof. Patrick Bernier, and finished construction of a high precision Seivert's apparatus.

In 1999 we developed a simple 3-step purification technique which could prepare SWNTs in greater than 98 wt% purity[19,20]. A thermal gravimetric analysis (TGA) method was developed to allow the accurate determination of nanotube wt% contents in carbon soots. We also established an ultrasonic process for cutting purified laser-generated materials. This advance was necessary since laser-produced tubes were found to be unresponsive to the oxidation methods that successfully opened arc-generated tubes. TPD spectroscopy demonstrated that purified cut SWNTs adsorbed between 3.5 – 4.5 wt% hydrogen under ambient conditions in several minutes and that the adsorbed hydrogen was effectively "capped" by CO_2

In 2000 we presented the details of an ultrasonic cutting procedure and showed that, when optimized, hydrogen storage densities up to 7 wt% can be achieved[21]. Infrared absorption spectroscopy measurements on pristine and H_2-charged samples indicated that no C-H bonds are formed in the hydrogen adsorption process. First neutron scattering measurements of hydrogen adsorbed on SWNTs were performed through collaboration with researchers at NIST and the University of Pennsylvania[22]. We also developed methods to tune SWNT diameters during synthesis[23] so that mechanistic aspects of H_2 storage could be probed, and learned how to de-tangle and organize individual tubes to form "superbundles"[24].

Last year we reaffirmed accurate calibrations for our TPD and volumetric apparatus using three different hydride standards (Pd, Ti and Ca)[10]. In all cases the two systems agreed within ± 5%. Materials generated with an alexandrite laser did not have the same high hydrogen storage capacities even when all of the same sample purification, cutting and activation steps were taken. We probed the differences between the Nd:YAG and alexandrite generated materials using two-color Raman spectroscopy and found that Nd:YAG materials contained a mixture of semi-conducting and metallic nanotubes while alexandrite materials contained predominantly metallic tubes. Because the Nd:YAG grown samples yielded high hydrogen adsorption capacities on a more regular basis, we performed a laser synthesis study with the alexandrite laser in which the production of metallic versus semiconducting SWNTs was investigates as a function of laser peak pulse power. We established that semiconducting tubes are produced at higher density with higher peak powers, and improved our ability to produce SWNTs with specific diameter and chirality distributions.

This year we used our capability to produce tailored SWNT distributions with an alexandrite laser to prepare samples that were similar in both size and type to those produced with the Nd:YAG laser. Although we have demonstrated high hydrogen storage capacities using tailored alexandrite materials, we are once again having difficulty making high hydrogen storage capacity samples in a repeatable fashion. This may be attributed the lack of control in the current cutting and alloy incorporation process. The degree of tube cutting and how, where and in what form the metal particles are incorporated vary even when identical cutting conditions are employed. Because it is desirable to have independent control over both cutting and metal incorporation, we have developed a controllable cutting technique that does not simultaneously

incorporate a metal hydride alloy. We have also developed a Raman spectroscopy technique that measures the extent of cutting in a given sample and have demonstrated that similar degrees of cutting are achieved for identical conditions with the new cutting method of discrete sizes.

Experimental

Pulsed Laser Synthesis of SWNTs

SWNT materials are produced with an alexandrite laser (755 nm). Targets are made by pressing graphite powder doped with 0.6 at% each of Co and Ni in a 1 1/8" inch dye at 20,000 psi. Laser syntheses are performed at 1200 °C with 500 torr Ar flowing at 100 sccm. The laser may be operated in a free-running mode with average powers varying from ~20 - 500 W/cm^2. The free running mode consists of ~ 1 ns pulses which are ≤ 1 ns apart and are produced in packets of ~ 1μs inside a 100 μs train repeated at 10 Hz. The effective pulse width is ~1 μs. For free running laser vaporization, crude soots may be produced at rates of 10-200 mg/hr depending on the laser power density. The alexandrite laser may be operated at 10 Hz and a constant average power while the laser pulse width is tuned to a value between 100 ns and 2.5 μs. This capability enables the effect of peak pulse power on SWNT size and type to be determined and controlled.

Purification of Laser-generated SWNTs

Approximately 80 mg of laser–generated crude is refluxed in 60 ml of 3M HMO3 for 16 h at 120 °C. The solids are collected on a 0.2 μm polypropylene filter in the form of a mat and rinsed with deionized water. After drying, an ~ 82 wt% yield is obtained. The weight lost is consistent with the digestion of the metal and an additional ~ 12 wt% of the carbon impurities. The carbon mat is then oxidized in stagnant air at 550 °C for 10 min., leaving behind pure SWNTs. The variable pulse-width capability enables a range of peak pulse powers to be obtained with a constant energy density per pulse. High peak pulse powers lead to bulk materials that are difficult to purify due to high concentrations of ablated graphite particles. At low peak pulse powers, the metal-doped graphite target is simply annealed by the laser pulses. As a result, the raw material has a high metal concentration and is produced at a very low rate. When care is taken to remain in a vaporization regime during synthesis, materials which are > 98 wt% pure may be obtained.

Cutting of Laser-generated SWNTs

In the ultrasonic cutting method, 2-3 mg samples are sonicated in 20 ml of 4M HNO_3 with a high-energy probe for times ranging from 10 minutes to 24 hrs at powers ranging from 25 – 250 W/cm^2. Following cutting, the very long nanotube ropes found after purification[20] are cut and re-organized. This large-scale cutting is consistent with the generation of cuts and defects as has been observed by others[25-27]. Also the cutting process incorporates metal particles ranging in size from several nanometers to several microns in the SWNT samples. X-ray patterns of the particles in the cut samples are consistent with an alloy of nominal composition $TiAl_{0.1}V_{0.04}$ as expected for disintegration of the ultrasonic probe.

Unfortunately this cutting method cannot be very well controlled. Differing degrees of cutting, amounts of metal, and metal particle sizes are found in processed samples even with careful control of external parameters such as sonication time, sonication power, acid concentration, hydrodynamics, etc. The variability in the process leads to variability in the performance of the

final materials, with storage capacities on the tube fraction ranging from 0 to 8 wt%. Controlled cutting of carbon single-wall nanotubes has been achieved via a new dry cutting method that does not employ ultrasonication.

Temperature Programmed Desorption

Details of the ultra high vacuum (UHV) chamber employed for the TPD studies have been reported previously[1,2]. Briefly, carbon samples weighing ~1 mg are placed in a packet formed from 25 μm thick platinum foil and mounted at the bottom of a liquid nitrogen cooled cryostat. The packet is resistively heated with a programmable power supply. Pinholes in the foil enable gas diffusion into and out of the packet. An ion gauge and a capacitance manometer were employed to monitor pressure. Gas exposures are controlled with a variable conductance leak valve. Isolation gate valves separate the sample compartment during high-pressure gas exposures. A mass spectrometer measures species with an m/e up to 300 a.m.u. and insures that only hydrogen is involved in adsorption/desorption cycles. The instrument is easily calibrated[28] by thermally decomposing known amounts of CaH_2. The amount of evolved hydrogen is linear with the weight of decomposed CaH_2, and the calibrations were performed with amounts of CaH_2 that were selected to yield a TPD signal similar to that measured with SWNT samples. The TPD system was also calibrated with Pd and Ti hydrides. All three hydrogen standards have been confirmed with the Seivert's volumetric technique and are in agreement within ±5%. Prior to hydrogen adsorption studies SWNT samples are initially degassed by heating in a vacuum of ~ 10^{-7} torr to 823 - 973 K at 1 K/s. The sample temperature is measured with a thin thermocouple spot-welded to the platinum packet. Room temperature H_2 exposures for ~ 1 minute at pressures between 10 and 500 torr saturate the hydrogen adsorption. Capacity determinations in the TPD are done by cooling the sample to 130 K prior to evacuation of the chamber.

Raman Spectroscopy

Raman spectroscopy is performed using ~7 mW of the 488 nm line of an Ar ion laser and ~9 mW of the 632.8 nm line of a HeNe laser. The scattered light is analyzed with a Jobin Yvon 270M spectrometer equipped with a liquid-nitrogen cooled Spectrum One CCD and a holographic notch filter. A 2400 grooves/mm grating is employed at 488 nm. A 1200 grooves/mm grating is employed at 632.8 nm in order to observe the spectral range of interest. A Nikon 55 mm camera lens is employed both to focus the beam on the sample to a ~0.25 mm^2 spot and to collect the Raman scattered light. At 488 nm a resolution of 2-4 cm^{-1} was measured across the entire range with Oriel spectral calibration lamps. The resolution is decreased by approximately a factor of two for the spectra obtained at 632.8 nm. Averaging three 30 s scans is sufficient to obtain high intensity, well-resolved Raman spectra.

Results and Discussion

Controlled Laser-Production of Tailored SWNT Size and Type Distributions

Last year we performed a detailed study and established that semiconducting tubes are produced at higher density when high laser peak pulse powers are employed. Also, as the laser peak pulse power increases, the SWNT diameter distributions shift to smaller diameters[23,29]. Using these two findings together we are able to produce nanotube diameter and type distributions with the alexandrite laser that are nearly identical to those produced with the Nd:YAG laser. Laser-generated single-wall carbon nanotubes typically range in diameter between ~0.8 – 1.6 nm. SWNTs also may be either metallic or semiconducting depending on

the tube chirality. The Raman modes of SWNTs are resonantly enhanced with different tubes being at resonance for different wavelengths of excitation. For this SWNT size regime, semiconducting tubes are predominantly excited at 488 nm and both metallic and semiconducting nanotubes are excited at 632.8 nm[30]. Figure 1 displays the Raman spectra in the radial breathing mode region for a) a sample produced in a free running Nd:YAG synthesis that had an SWNT adsorption capacity of ~7 wt%, and b) a sample produced in a controlled-pulse alexandrite synthesis. The Raman frequencies observed for the SWNT radial breathing modes are diameter dependent with the smaller tubes appearing at higher frequency[31]. The alexandrite synthesis was performed with a power density of ~21 W/cm^2 and a 200 ns pulse width corresponding to a peak pulse power of 10.5 MW/cm2. Note the similarity between the Raman spectra of Fig. 1 a) and b) indicating that for an alexandrite peak pulse power of 10.5 MW/cm2, SWNT size and type distributions are nearly identical to those produced with the Nd:YAG. Subsequent syntheses with the same peak power showed that the production of this SWNT size and type distribution is highly reproducible.

Poor Repeatability of High Hydrogen Adsorption Capacities

SWNT materials were activated for hydrogen storage with an ultrasonic treatment that cuts the pure tubes and simultaneously incorporates a metal hydride alloy having a composition of $TiAl_{0.1}V_{0.04}$[6,8,9]. The hydride alloy accounts for a portion of the hydrogen storage capacity of the alloy/nanotube composite material that is formed. Assuming that the Ti fraction of the alloy can be hydrided to a stoichiometry of TiH_2, the alloy would have a theoretical capacity of 2.48 wt%. The theoretical maximum value for hydrogen storage on the $TiAl_{0.1}V_{0.04}$ alloy is 3.44 wt%. Several experimental investigations report a maximum capacity of only ~2.99 wt% under similar temperature and pressure conditions to those employed here.[32-34] We generated fragments of the ultrasonic probe by running the probe for 16 hrs in 4M HNO_3 without the addition of SWNTs. The generated particles exhibited X-ray patterns consistent with the alloy found in the SWNT samples following ultrasonic probe treatment. The probe-generated form of the $TiAl_{0.1}V_{0.04}$ sample exhibited ~ 2.5 wt% hydrogen adsorption as measured by both TPD and volumetric techniques.

Figure 2 displays a plot of hydrogen storage capacity versus alloy metal content for numerous purified SWNT samples that were treated with the ultrasonic probe process. Among these samples are several tailored alexandrite materials produced at a laser peak power of 10.5 MW/cm^2. The metal contents were determined by combusting the carbon fraction in flowing air and accounting for the oxidation of the metals. Lines have been drawn as a guide to the eye to show the expected hydrogen storage capacity based on the content of the $TiAl_{0.1}V_{0.04}$ alloy if the alloy hydrogen storage density were 3.48, 2.99, or 2.5 wt%. It is apparent in Fig. 2 that the hydrogen adsorption on many of the NREL samples may be explained fully by adsorption on the incorporated alloy. However, approximately one-half of the samples show hydrogen adsorption capacities that are too high to be explained by the presence of the alloy alone. These data indicate that the SWNTs have been activated for hydrogen storage. In fact, in many cases the adsorption capacities of the SWNTs are quite significant. For example, the adsorption capacity on a sample that was sonicated for 16 hrs at 50 W/cm^2 is 6.5 wt%. This sample contains ~15 wt% $TiAl_{0.1}V_{0.04}$. Assuming that the alloy in the SWNT sample behaves like the pure probe-generated alloy sample, the hydrogen uptake on the SWNT fraction is ~ 7.2 wt%. Figure 2 also displays data from a recent paper by Hirscher et al. (MPI; black circles and diamonds)[8]. These researchers performed experiments similar to ours using arc-discharge SWNTs and diamond materials.

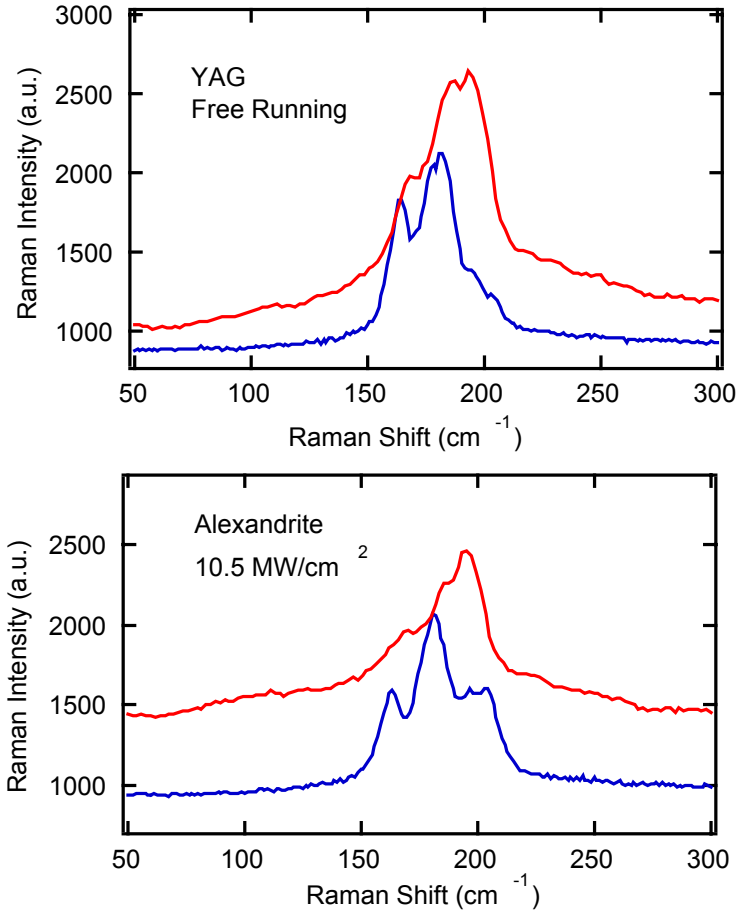

Figure 1: Raman spectra in the radial breathing mode region for a) a Nd:YAG-produced sample with a H_2 adsorption capacity of ~7 wt%, and b) a sample produced with the alexandrite laser operating with a 200 ns pulse width at a peak pulse power of 10.5 MW/cm^2. The red curves are for Raman excitation at 632.8 nm and show the SWNT size distribution for excited metallic and semiconducting tubes. The blue curves were obtained at 488 nm and show predominantly semiconducting tubes.

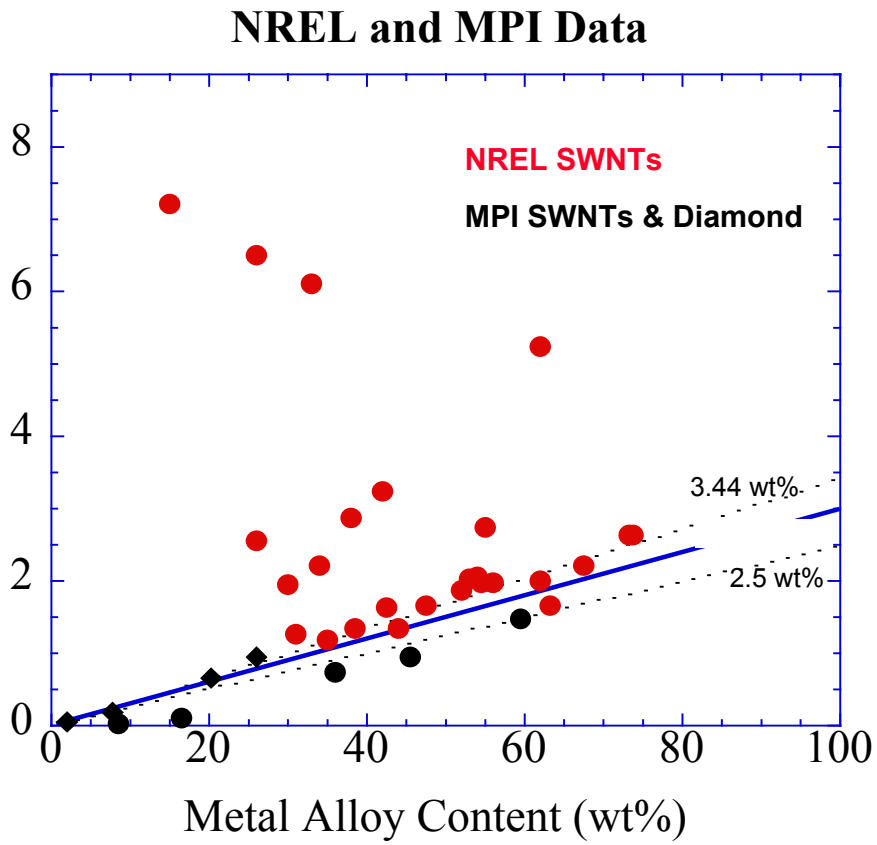

Figure 2: Plot of total sample hydrogen wt% content versus metal alloy content for SWNT samples following high energy sonication in HNO_3 with an ultra sonic probe. Data generated at NREL and from reference 8 are shown. Lines are drawn as a guide to the eye to show the anticipated hydrogen storage based on metal alloy content alone.

Figure 3 shows the same NREL data presented in Figure 2 plotted with the Y-axis displaying the hydrogen storage capacity of the SWNT fraction of the sample with the assumption that the alloy portion stores hydrogen at 2.99 wt%. The data is consistent with SWNTs that have hydrogen storage capacities between 0-8 wt%, with ~ 8 wt% being a maximum value independent of the amount of $TiAl_{0.1}V_{0.04}$ alloy that is present. Significant hydrogen storage capacities on the SWNT fractions of the tailored alexandrite materials were sometimes observed. However, the hydrogen storage capacity of these samples could often be explained by the presence of the metal alloy.

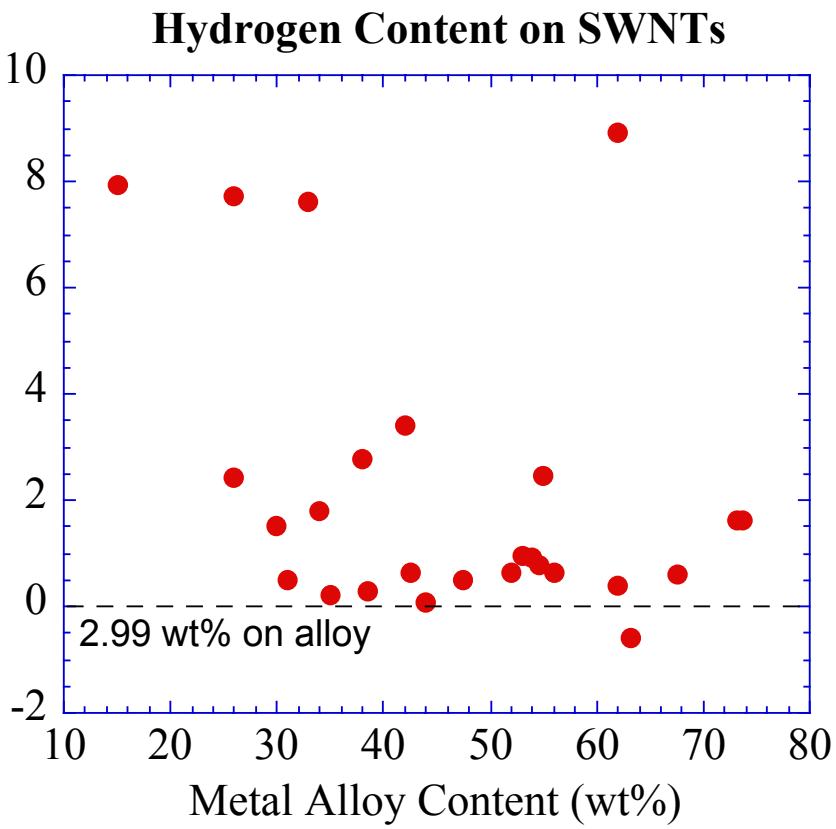

Figure 3: NREL data from Figure 2 plotted according to the following expression:
$(1 - X_{alloy}) * wt\% H_{SWNT} = wt\% H_{total} - (X_{alloy} * wt\% H_{alloy})$
where $wt\% H_{alloy} = 2.99$ wt% and X_{alloy} is the weight fraction of alloy in the sample.

The hydrogen storage capacities may vary dramatically even for nanotube samples with controlled size and type distributions. What then is the cause of these variations? One possible explanation is that the amount of destruction to the SWNTs during the ultrasonic process is sometimes rather extreme. For some of the data points in Fig. 2 that fall on the line corresponding to the metal hydride adsorption capacity, the nanotubes were almost completely destroyed leaving behind only graphitic particles and amorphous carbon. TEM images of the sonicated SWNT materials prepared by Hirscher et al.[8] also showed a significant degree of damage. In our experiments there are numerous examples of ultrasonically treated samples where the nanotubes appeared cut but not significantly damaged, and the SWNT hydrogen storage capacities were still found to be quite low. For some of these low SWNT hydrogen storage capacity samples, the majority of the incorporated metal alloy particles were quite large, ~1μ in diameter. Samples that had higher SWNT storage capacities generally contained smaller metal alloy particles that were several nanometers in diameter. These results suggest that the manner in which alloy particles are incorporated may be important. Small $TiAl_{0.1}V_{0.04}$ particles capable of intimate contact with the SWNTs may be necessary for activating the tubes for hydrogen storage. The dramatic variations in cutting and alloy incorporation occur even when the external parameters such as sonication time, sonication power, acid concentration and hydrodynamics are carefully controlled.

Development of Controlled Cutting Method Without Metal Hydride Incorporation

The ultrasonic activation method provides two distinct functions: cutting and metal alloy incorporation. However, the sonication process does not provide for detailed or independent control of either one. The variability in the process leads to variability in the performance of the final materials, with storage capacities on the tube fraction ranging from 0 to 8 wt.%. Consequently, we have focused on developing cutting method that can be controlled and are not coupled to the metal introduction process.

Controlled cutting of carbon single-wall nanotubes has been achieved via a new dry cutting method that does not employ ultrasonication. Unfortunately, we cannot reveal the details of the process at this time. Transmission electron microscopy analyses and Raman spectroscopy show that significant cutting occurs without extensive damage to the SWNTs. Figure 4 shows a TEM image of purified single-wall carbon nanotubes that were cut with the new cutting technique. Prior to cutting the tubes were tens to hundreds of microns in length, and it was difficult to discern nanotube ends. Numerous blunt ends are clearly observed, and many of the tubes are < 1 micron in length. Also in spite of the dramatic cutting, no evidence of nanotube destruction is observed.

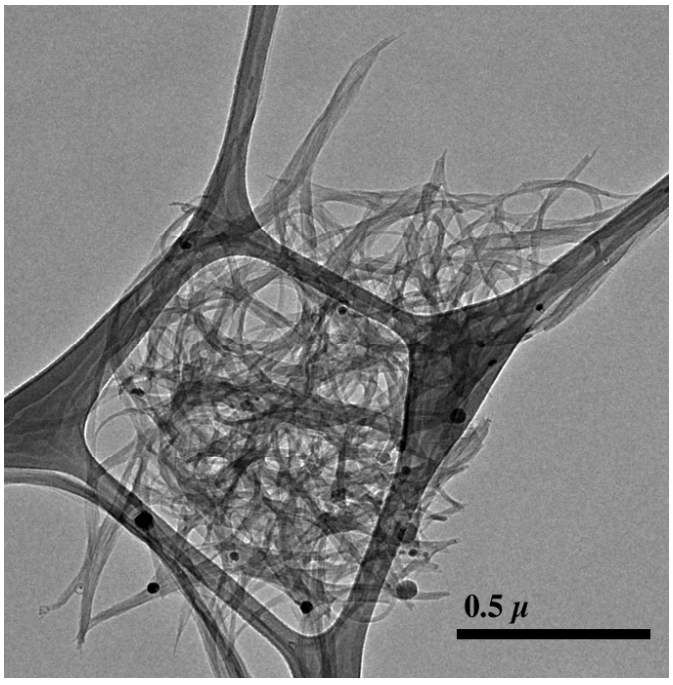

Figure 4: Transmission electron micrograph (TEM) showing cut SWNTs produced by a new cutting process that does not utilize ultrasonication. The dark lattice in the background is the TEM sample grid.

The hydrogen storage capacities of samples obtained by this cutting method were evaluated with temperature programmed desorption and volumetric techniques. Figure 5 displays hydrogen TPD spectra of a purified SWNT sample and an SWNT sample cut with the new method. Hydrogen exposures were at room temperature and 500 torr for several minutes, and the samples were then cooled in the presence of the gas. The TPD spectra of both samples contain a hydrogen desorption peak at ~-135 ˚C which can be attributed to the normal physisorbed hydrogen which is seen for activated carbons. The spectrum of the cut sample additionally shows a hydrogen desorption peak at ~65 ˚C, revealing the presence of hydrogen that is stabilized at ambient temperatures. This signal is similar to the one we reported previously for arc-discharge SWNTs[1], but it occurs at a temperature which is ~65 degrees higher. This is the first time we have been able to observe high-temperature adsorbed hydrogen on laser-generated materials without using the sonication activation process. Optimization of the process and the subsequent incorporation of catalytic metallic species will be explored in the future to determine if high-temperature, high-storage capacity materials may be prepared in a reproducible manner. The large increase in the magnitude of the low-temperature desorption signal after cutting may be due to the fact that the bundled SWNTs are more disordered following the cutting process.

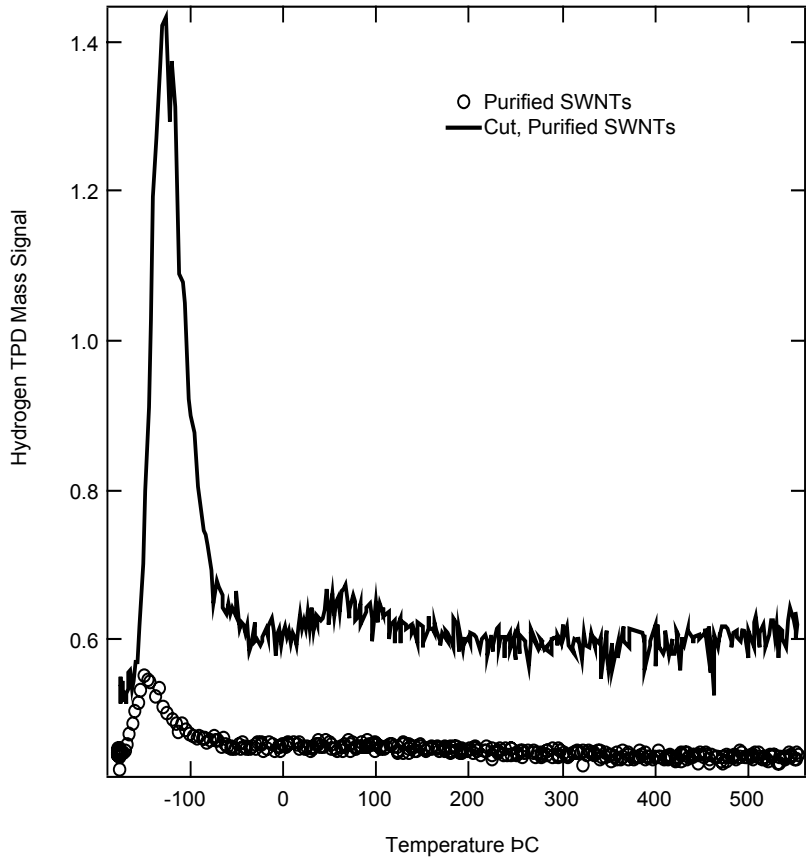

Figure 5: Temperature programmed desorption spectroscopy of purified SWNT materials before and after dry cutting process. The signal at 65 °C for the cut sample is similar to the one we reported previously for arc-discharge SWNTs[1], but it occurs at a temperature which is ~65 degrees higher.

A Simple Method to Determine Degree of SWNT Cutting

TEM analysis provides only a qualitative estimate of the degree of SWNT cutting. In order to establish if a relationship exists between cutting and the hydrogen storage capacities it is necessary to develop a method to quantify the degree of cutting obtained in macroscopic SWNT samples. A direct measurement of the degree of cutting will enable a better understanding of the hydrogen adsorption mechanism. We have developed a method to ascertain the degree of cutting using an analysis of the SWNT Raman mode at 1350 cm^{-1}. This band has been labeled the nanotube D-band, and we have shown that the intensity of this band increases when the nanotubes are cut and new defects are introduced. Figure 6 shows the Raman spectra of a purified SWNT sample and the same sample following the new cutting process. The spectra are normalized to the SWNT G-band Raman feature at 1593 cm^{-1}. The G-band serves as a useful spectral feature for normalization because it does not change in intensity with cutting or the introduction of new defects. An increase of ~ 25% is clearly observed for the D-band intensity in the spectrum of the cut SWNTs in Fig. 6. The details of this new Raman method for evaluating the degree of cutting in various SWNT samples have been submitted to Physical Review B. Figure 7 displays the D-band / G-band (D/G) intensity ratio for several different initial samples and the same samples following identical controlled cutting procedures. The fact that the absolute magnitude of the increase in the D/G ratio is very nearly the same for all three samples after identical cutting procedures suggests that the D/G ratio is correlated with the degree of cutting. Further development of this method to quantify the cutting process should enable a better understanding of the hydrogen storage mechanism and ultimately allow the SWNT hydrogen storage capacities to be reproducibly optimized.

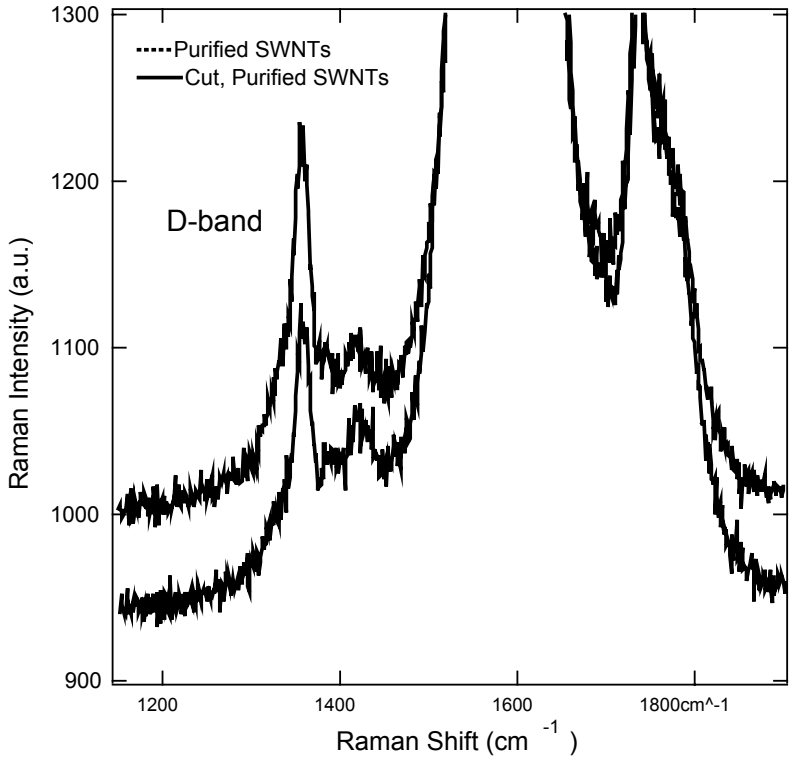

Figure 6: Raman spectra at 488 nm for a purified and a purified/cut sample. The spectra are normalized to the G-band intensity at ~ 1593 cm^{-1}, which is off-scale. The D-band intensity is enhanced relative to the G-band intensity in the cut sample.

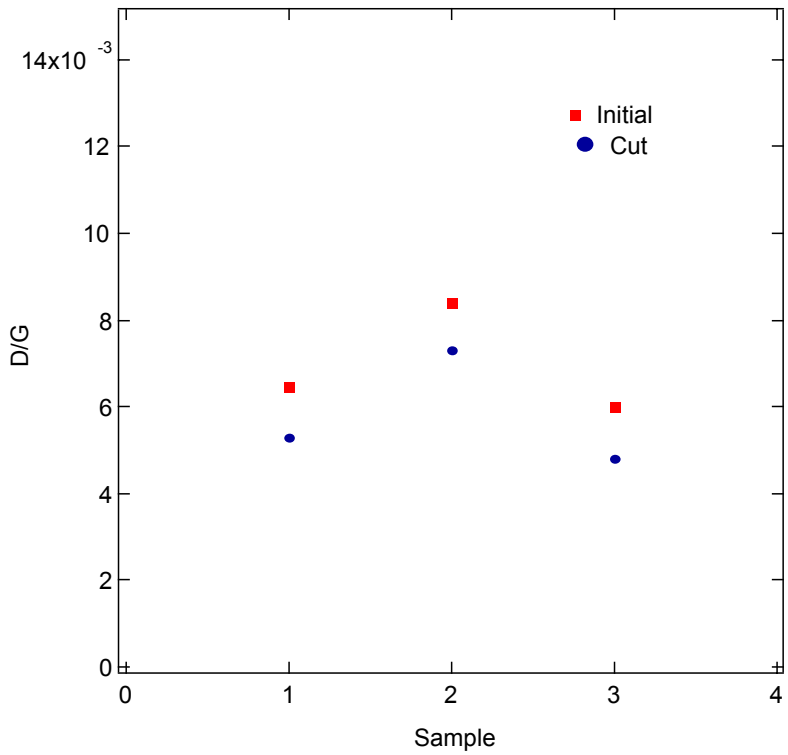

Figure 7: The ratio of the D-band intensity to the G-band intensity for a few samples before and after cutting. The D/G intensity ratio increases by a fixed amount after the same cutting procedures were applied.

Conclusions / Future Work

Hydrogen storage in carbon single-wall nanotubes has become the focus of numerous research groups in the world. However, obtaining activated SWNT hydrogen storage materials with highly reproducible adsorption capacities has not yet been achieved. One reason for this may be that hydrogen storage is only optimized for a very specific and narrow distribution of SWNTs of distinct types and diameters. We have established laser synthesis conditions that reproducibly produce SWNTs with size and type distributions that were previously found to have optimal hydrogen storage capacities of ~7 wt.%.

Unfortunately even when these optimized SWNT hydrogen storage materials are activated with an ultrasonic cutting procedure, they do not always display significant or repeatable hydrogen storage capacities. The ultrasonic cutting process simultaneously cuts the SWNTs and incorporates a metal hydride alloy. Both may be important to achieve high room-temperature hydrogen storage capacities. However, neither is well-controlled in the ultrasonic cutting process. Even when the external parameters such as sonication time, sonication power and acid concentration are identical, the degree of nanotube cutting can range from negligible to nearly complete destruction. Similarly the size of the incorporated metal particles can range from several microns to several nanometers. Consequently, we have developed a new controlled dry cutting method that non-destructively cuts the SWNTs without incorporating a metal hydride alloy.

In order to establish the degree of control achieved with the new cutting method, we have developed a new Raman spectroscopy-based technique that promises to allow the extent of SWNT cutting to be quantified. The method is based on monitoring the intensity of the SWNT Raman D-band, which we have shown to be correlated to the number of defects (i.e. ends) in a specific nanotube sample. We have used this Raman technique to show that when identical conditions are employed to presumably achieve similar degrees of cutting, the ratio of the D-band to the G-band increases by a fixed amount.

In the future we will correlate the degree of SWNT cutting with hydrogen storage capacities in order to understand the hydrogen adsorption mechanism more completely. We will also probe possible adsorption pathways in order to explain why only specific nanotubes appear to be optimal for hydrogen storage applications. We believe that the optimal tubes for hydrogen storage may allow adsorption to occur with partial charge transfer from the nanotube to the adsorbed H2 molecule. Finally, we will develop a method for the controlled incorporation of metal catalyst particles of discrete sizes and in specific locations so that SWNT hydrogen storage capacities may be reproducibly optimized.

References

(1) Dillon, A. C.; Jones, K. M.; Bekkedahl, T. A.; Kiang, C. H.; Bethune, D. S.; Heben, M. J. *Nature* **1997**, *386*, 377.

(2) Dillon, A. C.; Bekkedahl, T. A.; Cahill, A. F.; Jones, K. M.; Heben, M. J. "Carbon Nanotube Materials for Hydrogen Storage" In *Proceedings of the U.S. DOE Hydrogen Program Review* Coral Gables, FL, 1995; pp 521.

(3) Carpetis, C.; Peschka, W. *Int. J. Hydrogen Energy* **1980**, *5*, 539.

(4) Schwarz, J. A. "Modification Assisted Cold Storage (MACS)" In *contract report to Brookhaven National Laboratories, contract # 186193-S.*

(5) Schwarz, J. A. "Activated Carbon Based Storage System" In *Proceedings of the 1992 DOE/NREL Hydrogen Program Review* Honolulu, HI., 1992; pp 271.

(6) Dillon, A. C.; Heben, M. J. *Appl. Phys. A* **2001**, *72*, 133.

(7) Zandonella, C. *Nature* **2001**, *410*, 734.

(8) Hirscher, M.; Becher, M.; Haluska, M.; Dettlaff-Weglikowska, U.; Quintel, A.; Duesberg, G. S.; Choi, Y.-M.; Downes, P.; Hulman, M.; Roth, S.; Stepanek, I.; Bernier, P. *Appl. Phys. A* **2001**, *72*, 129–132.

(9) Heben, M. J.; Dillon, A. C.; Gennett, T.; Alleman, J. L.; Parilla, P. A.; Jones, K. M.; Hornyak, G. L. *Proc. Mat. Res. Soc.* **2000**, *663*, in press.

(10) Dillon, A. C.; Gilbert, K. E. H.; Alleman, J. L.; Gennett, T.; Jones, K. M.; Parilla, P. A.; Heben, M. J. "Carbon Nanotube Materials for Hydrogen Storage" In *Proceedings of the U.S. D.O.E Hydrogen Program Review* Baltimore, MD, 2001.

(11) Heben, M. J. "Carbon Nanotubules for Hydrogen Storage" In *Proceedings of the 1993 DOE/NREL Hydrogen Program Review* Cocoa Beach, FL, 1993; pp 79.

(12) Pederson, M. R.; Broughton, J. Q. *Physical Review Letters* **1992**, *69*, 2689.

(13) Bekkedahl, T. A.; Heben, M. J. "Advanced materials for hydrogen storage: Carbon nanotubules" In *Proceedings of the 1994 DOE/NREL Hydrogen Program Review* Livermore, CA., 1994; pp 149.

(14) Dillon, A. C.; Jones, K. M.; Heben, M. J. "Carbon nanotube materials for hydrogen storage" In *Proceedings of the 1996 DOE/NREL Hydrogen Program Review* Miami, FL, 1996.

(15) Dillon, A. C.; Parilla, P. A.; Jones, K. M.; Webb, J. D.; Landry, M. D.; Heben, M. J. "Carbon nanotube materials for hydrogen storage" In *Proceedings of the 1997 DOE/NREL Hydrogen Program Review*; National Renewable Energy Laboratory: Herndon, VA, 1997; pp 237.

(16) Dillon, A. C.; Landry, M. D.; Webb, J. D.; Jones, K. M.; Heben, M. J. "The Oxidation and Reduction of Single-wall Carbon Nanotubes" In *Recent Advances in the Physics and Chemistry of Fullerenes and Related Materials*; Ruoff, R. S., Kadish, K. M., Eds.; Electrochemistry Society Inc.: Montreal, Canada, 1997; Vol. 4; pp 916.

(17) Guo, T.; Nikolaev, P.; Thess, A.; Colbert, D. T.; Smalley, R. E. *Chemical Physics Letters* **1995**, *243*, 49.

(18) Dillon, A. C.; Parilla, P. A.; Jones, K. M.; Riker, G.; Heben, M. J. "Carbon Nanotube Materials for Hydrogen Storage" In *Proceedings of the 1998 U.S. DOE Hydrogen Program Review* Alexandria, VA, 1998.

(19) Dillon, A. C.; Gennett, T.; Alleman, J. L.; Jones, K. M.; Parilla, P. A.; Heben, M. J. "Carbon Nanotube Materials for Hydrogen Storage" In *Proceedings of the 1999 DOE/NREL Hydrogen Program Review* Golden, CO, 1999.

(20) Dillon, A. C.; Gennett, T.; Jones, K. M.; Alleman, J. L.; Parilla, P. A.; Heben, M. J. *Advanced Materials* **1999**, *11*, 1354.

(21) Dillon, A. C.; Gennett, T.; Alleman, J. L.; Jones, K. M.; Parilla, P. A.; Heben, M. J. "Carbon Nanotube Materials for Hydrogen Storage" In *Proceedings of the 2000 DOE/NREL Hydrogen Program Review* San Ramon, CA, 2000.

(22) Brown, C. M.; Yildirim, T.; Neuman, D. A.; Heben, M. J.; Gennett, T.; Dillon, A. C.; Alleman, J. L.; Fischer, J. E. *Chem. Phys. Lett.* **2000**, *329*, 311.

(23) Dillon, A. C.; Parilla, P. A.; Alleman, J. L.; Perkins, J. D.; Heben, M. J. *Chem. Phys. Lett.* **2000**, *316*, 13.

(24) Gennett, T.; Dillon, A. C.; Alleman, J. L.; Hassoon, F. S.; Jones, K. M.; Heben, M. J. *Chem. of Mat.* **2000**, *12*, 599.

(25) Shelimov, K. B.; Esenaliev, R. O.; Rinzler, A. G.; Huffman, C. B.; Smalley, R. E. *Chem. Phys. Lett.* **1998**, *282*, 429.

(26) Liu, J.; Rinzler, A. G.; Dai, H.; Hafner, J. H.; Bradley, K. R.; Boul, P. J.; Lu, A.; Iverson, T.; Shelimov, K.; Huffman, C. B.; Roderiguez-Macias, F.; Shon, Y.-S.; Lee, T. R.; Colbert, D. T.; Smalley, R. E. *Science* **1998**, *280*, 1253.

(27) Lu, K. L.; Lago, R. M.; Chen, Y. K.; Green, M. L. H.; Harris, P. J. F.; Tsang, S. C. *Carbon* **1996**, *34*, 814.

(28) Wang, J.; McEnaney, B. *Thermochimica Acta.* **1991**, *190*, 143.

(29) Dillon, A. C.; Alleman, J. L.; Gennett, T.; Jones, K. M.; Parilla, P. A.; Heben, M. J. *(in preparation)* **2001**.

(30) Pimenta, P.; Marucci, M.; Brown, S. D. M.; Matthews, M. J.; Rao, A. M.; Eklund, P. C.; Smalley, R. E.; Dresselhaus, G.; Dresselhaus, M. S. *Journal of Materials Research* **1998**, *13*, 2396.

(31) Rao, A. M.; Richter, E.; Bandow, S.; Chase, B.; Eklund, P. C.; Williams, K. A.; Fang, S.; Subbaswamy, K. R.; Menon, M.; Thess, A.; Smalley, R. E.; Dresselhaus, G.; Dresselhaus, M. S. *Science* **1997**, *275*, 187.

(32) Davis, J. W.; Smith, D. L. *J. Nuc. Mat.* **1979**, *85*, 71.

(33) Jiao, J.; Seraphin, S. *Journal of Materials Research* **1998**, *13*, 2438.

(34) S. Ishiyama; K. Fukaya; M. Eto; Miya, N. *Journal of Nuclear Science and Technology* **2000**, *37*, 144.